# Isotopic effects in low-energy lithium-hydrogen collisions

Andrey K. Belyaev* and Yaroslav V. Voronov
*Department of Theoretical Physics and Astronomy, Herzen University, St. Petersburg 191186, Russia*

(Received 10 February 2021; accepted 27 July 2021; published 13 August 2021)

The cross sections and rate coefficients for the inelastic processes of mutual neutralization, ion-pair formation, and (de)-excitation in lithium-hydrogen collisions are calculated based on the *ab initio* electronic structure [J. Phys. B: At. Mol. Opt. Phys. **32**, 81 (1999)] and the hopping probability current method [Phys. Rev. A **88**, 052704 (2013)] for the nonadiabatic nuclear dynamics. For each given set of collisional parameters, calculations of the probability current evolution were repeated $2.621\,44 \times 10^9$ times, and this leads to a high accuracy of the inelastic state-to-state transition probabilities, the cross sections, and finally, the rate coefficients. The isotopic effects on the processes in collisions $^6$Li / $^7$Li + H/D/T, where (H/D/T) represents hydrogen, deuterium, and tritium, for different isotopes are studied. In addition, the deexcitation resonance processes $^{6,7}$Li$(2p \rightarrow 2s)$ + H/D/T were treated by the branching probability current method. It is found that the isotopic effects are different for different collisional partners and for different electronic states involved into a process, varying from negligible effects for high-lying Li states to strong effects for low-lying Li states. The resonance transition process is one with the strongest isotopic effects: replacing H by T changes the rate coefficient by up to four orders of magnitude. Unfortunately, there is no experimental data for the processes with strong isotropic effects, only for the processes with moderate effects, up to 60%.

DOI: 10.1103/PhysRevA.104.022812

## I. INTRODUCTION

Lithium (Li) is of particular importance in astrophysics. This chemical element was created in Big Bang nucleosynthesis, cosmic ray spallation, and stellar processes, see review [1] for atomic, molecular, and optical physics in the early Universe as well as Refs. [2–4] for lithium chemistry in the early universe. Information about lithium can help to solve some important problems, for instance, the cosmological lithium problems including both the primordial lithium problem [5] and the so-called Spite plateau problem (or the second lithium problem) [6] as well as radial migration, ages of stars, stellar clusters, and so on [7,8]. One of the most important is the primordial $^7$Li problem [9], consisting of the fact that $^7$Li is predicted by the standard Big Bang nucleosynthesis theory in a very small primordial production in the first minutes of the Universe at about ten orders of magnitude lower than hydrogen (H) and helium (He), but this small amount of lithium is still a factor of 3 to 4 greater than $^7$Li observations in the oldest stars although deuterium and $^4$He measurements agree well with the predictions, see Refs. [5,10–16] and very recent references therein. The prediction for the $^6$Li isotope is even lower with a not measurable tiny isotopic ratio of $^6$Li/$^7$Li being equal to $2.75 \times 10^{-5}$ [11]. On the other hand, $^6$Li can be produced by the interaction of energetic nuclei of Galactic cosmic rays with the nuclei of the interstellar medium. This production channel should increase the $^6$Li abundance and, hence, the isotopic ratio up to 1%. Other possible production channels might be nonstandard physics in the Big Bang or pregalactic origin. The recent analysis of the lithium profile of the primary star provides the ratio $^6$Li/$^7$Li = 8% with an upper limit $< 10\%$ [11]. One should also mention the second lithium problem related to the asymmetry of the $^7$Li doublet line at 670.8 nm produced by the presence of $^6$Li. Solutions of these and many other problems require accurate measurements or calculations of lithium abundances in stars. The calculations, in turn, rely in large part on accurate atomic data, both radiative and collisional ones.

The most accurate calculations of abundances are whose obtained from nonlocal thermodynamic equilibrium (NLTE) stellar atmosphere modeling. It has been recognized a long time ago that the main uncertainty in NLTE calculations is coming from the lack of quantum data on inelastic processes in collisions of a treated chemical element with hydrogen [17,18]. The matter of the fact is that the H-collisional rate coefficients have been estimated by the so-called classical Drawin formula [19], but later on it has been shown that the Drawin formula is not correct [20], leading to deviations from the rate coefficients obtained by full quantum calculations up to several orders of magnitude. Thus, reliable quantum data on inelastic processes in collisions of a treated chemical element with hydrogen are highly desired.

In addition to the aforementioned problems, there exist some open questions concerning different isotopes, even in the primordial lithium problem [5]. Another example is the existence of a $^6$Li plateau, which appears questionable after a reanalysis of three-dimensional NLTE stellar atmosphere modeling instead of a one-dimensional model for both $^6$Li and $^7$Li [7]. Again, accurate NLTE line formation analysis requires accurate rate coefficients for inelastic processes in lithium-hydrogen collisions for different isotopes.

*andrey.k.belyaev@gmail.com

 

Concerning inelastic lithium-hydrogen collisional processes needed for NLTE studies, isotopic effects should be studied, that is, influence of using different isotopes of both collision partners on partial rate coefficients for inelastic processes in $^6$Li / $^7$Li +H/D/T, where D and T represent deuterium and tritium, collisions should be investigated. Thus, in astrophysics there exists a high demand for quantum data on inelastic processes in lithium-hydrogen collisions for different isotopes of both lithium and hydrogen. Investigation of isotopic effects in inelastic lithium-hydrogen collisional processes is the goal of the present paper.

In addition to astrophysical importance, the isotopic effects in different collisions, in general, and in lithium-hydrogen collisions, in particular, are of interest in laboratory plasma physics, planetary ionospheres, in the chemistry, and so on. Moreover, these collisions are important from a fundamental point of view: Experimental studies of this kind of systems remain an important challenge [21]. Despite this, comparison of experimental and theoretical results gives an important test of both an experiment and a theory. For this reason, lithium-hydrogen collisions have been studied by both experimentally [21–24] and theoretically [21,25–28]. Investigations of these collisions continue up to present: Recently, experimental [21,24] and theoretical [21,28,29] data have been published, mainly for mutual neutralization processes in low-energy lithium-hydrogen collisions. So, there is an interest in isotopic effects not only in $^6$Li / $^7$Li, but also in H/D/T. Moreover, for NLTE stellar atmosphere modelings, one needs to know cross sections and rate coefficients for different isotopes not only for mutual neutralization, but also for excitation and deexcitation processes. This kind of information for (de)-excitation processes is currently unknown. Thus, the investigation of the isotopic effects for all kinds of processes in lithium-hydrogen collisions is the goal of the present paper. Throughout the paper, atomic units (au) ($m_e = e = \hbar = 1$) are used unless stated otherwise.

## II. BRIEF THEORY

Accurate determination of lithium abundances from NLTE modelings of stellar atmosphere spectra requires accurate rate coefficients of inelastic processes in lithium-hydrogen collisions. In general, this information could be derived from experimental measurements, but, in practice, experimental abilities are very limited, so the only real source to acquire collisional information is theoretical calculations. Obviously, the most accurate rate coefficients of inelastic collisional processes are those obtained by full quantum calculations. Unfortunately, full quantum calculations are still time consuming and, hence, performed only for a few chemical elements collided with hydrogen atoms or/and anions: Na [30,31], Li [26,27] (only mutual neutralization processes), Mg [32,33], and Ca [34]. Moreover, NLTE calculations typically require information about hundreds, thousands, and even $10^6$ state-to-state inelastic collisional processes,[1] which makes full quantum calculations not realistic. As such, more approximate, but still quantum and reliable model approaches are sufficient.

The most widely used framework to study atomic collisional processes is the Born-Oppenheimer approach. Within this approach the consideration is performed into two steps: (i) electronic structure calculations at fixed nuclei, and (ii) nonadiabatic nuclear dynamical treatment. A few quantum model approaches have been proposed within the Born-Oppenheimer approach for each step. They are as follows: various *ab initio* methods (the highest accuracy), various asymptotic methods including one from Ref. [35], the atomic and molecular orbitals based methods including one from [36,37], semiempirical methods including one from Ref. [38], the simplified model [39], etc., for electronic structure calculations, and the reprojection method (the highest accuracy) [40,41], various coupled channel equations methods, different nonadiabatic models including the Landau-Zener (LZ) and the Landau-Zener-Belyaev-Lebedev models [42], the probability current methods (branching or hopping) [35], the multichannel analytic approach [43,44], the simplified model, the perturbation theory, and so on for nonadiabatic nuclear dynamics. The quantum model approaches have been successfully applied to inelastic processes in collisions of various chemical elements with hydrogen, see, e.g., Refs. [35,45–47] and references therein. The calculated rate coefficients agree well with full quantum results (including *ab initio*), especially for inelastic processes with rate coefficients having the values in the range of $10^{-11}$–$10^{-7}$ cm$^3$ s$^{-1}$, that is, high and moderate values, see, e.g., Fig. 1 in Ref. [39].

A choice of a dynamical model for calculating inelastic transition probabilities, cross sections and rate coefficients depends to some extent on electronic structure calculations. If only asymptotic potentials are known, nonadiabatic transition probabilities, cross sections and rate coefficients can be estimated by asymptotic models, in practice, by the multichannel analytic approach, the simplified model, or the perturbation theory. In this case, there is no sense to accomplish more complicated and time-consuming dynamical calculations. In many cases asymptotic estimates are sufficient for NLTE modelings. If electronic structure is calculated with high accuracy by an *ab initio* method for the whole range of the internuclear distance, then more complicated and more accurate dynamical calculations can be performed, e.g., by the reprojection method, the branching or hopping probability current methods. These methods account not only for long-range nonadiabatic regions, but also for short- and intermediate-range regions, and this increases accuracy of nuclear dynamical calculations, especially for rates with low and intermediate values.

In the case of lithium-hydrogen collisions, the electronic structure has been calculated by the *ab initio* pseudopotential method [27], see that paper for description of the method for comparison of the calculated data with the experimental ones and for corrections of the potentials to improve them. The results of the calculations are given in the diabatic presentation for seven covalent and one ionic LiH($^1\Sigma^+$) molecular states listed in Table I. The diabatic representation allows one to obtain the electronic structure in the adiabatic representation.

[1] A state-to-state process from a given initial channel to a well-defined final channel is called a partial process.

TABLE I. LiH($j\ ^1\Sigma^+$) molecular states, the corresponding asymptotic scattering channels (atomic states), the asymptotic energies (in units of eV) with respect to the ground-state level, and the statistical probabilities for population of the molecular states.

| $j$ ($nl$) | Asymptotic scattering channels | Asymptotic energies (eV) | $p_j^{\rm stat}$ |
|---|---|---|---|
| 1 ($2s$) | Li($2s\ ^2S$) + H($1s\ ^2S$) | 0.0 | 0.2500 |
| 2 ($2p$) | Li($2p\ ^2P$) + H($1s\ ^2S$) | 1.8480 | 0.0833 |
| 3 ($3s$) | Li($3s\ ^2S$) + H($1s\ ^2S$) | 3.3738 | 0.2500 |
| 4 ($3p$) | Li($3p\ ^2P$) + H($1s\ ^2S$) | 3.8343 | 0.0833 |
| 5 ($3d$) | Li($3d\ ^2D$) + H($1s\ ^2S$) | 3.8795 | 0.0500 |
| 6 ($4s$) | Li($4s\ ^2S$) + H($1s\ ^2S$) | 4.3416 | 0.2500 |
| 7 ($4p$) | Li($4p\ ^2P$) + H($1s\ ^2S$) | 4.5223 | 0.0833 |
| Ionic | $Li^+(1s^2\ ^1S) + H^-(1s^2\ ^1S)$ | 4.6377 | 1.0 |

The paper [27] not only presents the results of the LiH electronic structure calculations, but also compares them with experimental data, e.g., with the observed vibrational spacings for the $A$ molecular state. The comparison shows good agreement, especially after corrections of the diabatic potentials. In particular, the ionic diabatic potential was shifted by 420 $cm^{-1}$ in order to reach the experimental value for the hydrogen electron affinity ($H^-$), and this shift improves the agreement of the calculated and the experimentally measured vibrational spacings for the $A$ state. It is known that this electron affinity error is the main source of the discrepancies in *ab initio* calculations involving $H^-$. In addition, Table II compares the available quantum chemical data from Refs. [21,27,48], that is, the asymptotic energies for the scattering channels, the positions of the long-range nonadiabatic regions, and maximum values of the corresponding nonadiabatic coupling matrix elements (NACME). One can see good agreement between these data, except for NACME for two uppermost-lying nonadiabatic regions. The source of these discrepancies is calculation of the two-electron wave function in $H^-$ with electron correlation, the same origin as one in calculation of the ionic potential in the long-range region. However, it turns out that these deviations are without much importance. From this analysis we assess the error of the calculated potentials being equal to $10^{-3}$ eV. Finally, one can make the conclusion that the quantum chemical data calculated in Ref. [27] are accurate and can be used for treating nonadiabatic nuclear dynamics not only at long-range, but also at short-range nonadiabatic regions.

The goal of the present paper is to study isotopic effects in lithium-hydrogen collision processes. There are two kinds of isotopic effects: (i) the effects related to nonadiabatic nuclear dynamics with different nuclear masses, and (ii) the effects related to mass-corrections (mass-polarization terms) to potential-energy curves as well as corrections of NACME due to changing of electron origins because of treating different isotope(s). The former effects are studied and discussed below; they determine the main isotopic effects. The situation with the latter is the following. (a) According to the strict formalism of a scattering problem within the Born-Oppenheimer approach, e.g., the reprojection method [40,41], the reduced masses used in the coupled-channel equations are different in an interaction region (molecular Jacobi coordinates, a reduced mass of an electron and all nuclei in the quasimolecule) and in asymptotic regions (state-specific scattering Jacobi coordinates, a reduced mass of an electron and an atomic nucleus; note different reduced masses in different scattering channels for heteronuclear systems). It seems that different reduced masses should result in different values of potentials in the asymptotic regions where they must match the one another. However, one should include into consideration the nonadiabatic corrections, that is, the matrix elements of the second derivative with respect to the internuclear distances [40]. In this case, the adiabatic potentials written in the molecular and in the atomic Jacobi coordinates are equal to each other in the asymptotic regions. Thus, the coupled-channel equations for the scattering problem in the time-independent Born-Oppenheimer approach should be solved in the molecular Jacobi coordinates with one reduced mass of an electron-nuclei system, and in the asymptotic region(s) these solutions should be matched to their asymptotic form(s) with another reduced mass(es), and the corresponding adiabatic effective potentials (including the radial second derivative matrix elements) should coincide with each other, see Ref. [40] for details. This conclusion holds for all isotopic combinations.

(b) Another fundamental feature of the Born-Oppenheimer approach is the dependence of NACME (both radial and

TABLE II. The comparison of the LiH($j\ ^1\Sigma^+$) asymptotic channel energies (in units of eV), the internuclear distances $R_c$ (in atomic units, a.u.) of the centers of the long-range nonadiabatic regions and the maximum values of radial NACME (in a.u.) at corresponding $R_c$.

| Asymptotic energies (eV) | Li($2s$) + H | Li($2p$) + H | Li($3s$) + H | Li($3p$) + H | Li($3d$) + H | Li($4s$) + H | Li($4p$) + H | $Li^+$+$H^-$ |
|---|---|---|---|---|---|---|---|---|
| Croft *et al.* [27] (present paper) | 0.0 | 1.8480 | 3.3738 | 3.8343 | 3.8795 | 4.3416 | 4.5223 | 4.6377 |
| NIST [48] | 0.0 | 1.8478 | 3.3731 | 3.8343 | 3.8786 | 4.3409 | 4.5216 | 4.6377 |
| Launoy *et al.*[21] (ACV5Z + G basis) | 0.0 | 1.8495 | 3.3721 | 3.8357 | 3.8770 | 4.3561 | | 4.639 |
| Positions of nonadiabatic regions, $R_c$ (a.u.) | | $2s$-$2p$ | | $2p$-$3s$ | $3s$-$3p$ | | $3p$-$3d$ | $3d$-$4s$ |
| Croft *et al.* [27] (present paper) | | 7.20 | | 11.30 | 22.05 | | 34.40 | 35.90 |
| Launoy [21] (ACV5Z+G) | | 7.19 | | 11.41 | 22.12 | | 34.05 | 35.97 |
| Max radial NACME (a.u.) | | $2s$-$2p$ | | $2p$-$3s$ | $3s$-$3p$ | | $3p$-$3d$ | $3d$-$4s$ |
| Croft *et al.* [27] (present paper) | | 0.22 | | 0.17 | 0.47 | | 1.08 | 3.69 |
| Launoy *et al.* [21] (ACV5Z + G) | | 0.21 | | 0.18 | 0.50 | | 1.24 | 2.04 |

rotational couplings but not adiabatic potentials) on the origin of electron coordinates [40]. The many-particle kinetic-energy operator has its simplest form in Jacobi coordinates when the electron coordinates are measured from a center of (fixed) nuclear mass. In this case, replacing one nucleus by its isotope changes a position of the center of nuclear mass, and, hence, this changes corresponding NACME, whereas the potentials remain unchanged. One of the consequences of this is the fact that some radial NACME remain nonzero in the asymptotic region.

(c) However, the usual practice is to use the electron mass instead of a reduced mass (an electron—an atomic nucleus and an electron—molecular nuclei). It turns out that the distinction between using of the electron mass and a reduced electron-nucleus mass is without much importance. We estimate the error of such replacement to be of $4 \times 10^{-3}$ eV, which is close to the error value obtained from the comparison of the calculated and experimental energies. Thus, this value is considered as the error for the calculated LiH potentials [27]. This error bar covers the scatter of asymptotic energy deviation as compared to the experimental data [48].

As shown below, the main isotopic effects in the treated processes occur due to nuclear dynamics. So, the approach to treat the nonadiabatic nuclear dynamics as accurately as possible is the central point of the present paper. Since the full quantum approach is still time consuming, a model approach is preferable. A known accurate electronic structure allows one to make use of more complicated but more accurate nuclear dynamics approaches. As such, nonadiabatic nuclear dynamical calculations can be accomplished by the deterministic branching or probabilistic hopping probability current methods. We choose the hopping probability current method[2] because this method requires adiabatic potentials only. It provides reliable data, especially for inelastic processes with large and moderate values of rate coefficients, the processes that are of main interest for applications, and the computational time is much shorter than for complete quantum calculations with a comparable accuracy.

The detailed description of the hopping probability current method is given in Refs. [28,45], so only the main idea of the method is described below. The key point of the method is an evolution of a probability current from a chosen initial scattering channel as a function of an internuclear distance $R$. Reaching a nonadiabatic region, a nonadiabatic transition probability to hop into another molecular state after a single traverse of the nonadiabatic region is calculated by means of the LZ model [49–51],

$$p = \exp\left(-\frac{\xi}{v}\right), \tag{1}$$

$v$ being a radial velocity at the center of a nonadiabatic region $R_c$ formed by adjacent states, and $\xi$ the Landau-Zener parameter. In practice, it is more convenient to use the adiabatic-potential-based formula [42] [the Belyaev-Lebedev (BL) formula], which expresses the LZ parameter $\xi$ in terms of the adiabatic energy splitting $Z = U_{\rm up} - U_{\rm down}$ and its second derivative $Z''$ with respect to $R$ at the center of the region,

$$\xi = \frac{\pi}{2\hbar}\sqrt{\frac{Z^3}{Z''}}\bigg|_{R=R_c}, \tag{2}$$

$U_{\rm up}$ and $U_{\rm down}$ being the adiabatic energies of two adiabatic adjacent states. Then a random number is generated and compared with $p$ in each nonadiabatic region reached by the probability current. From this comparison for each nonadiabatic region, a decision is made whether a probability current hops into another adiabatic molecular state or not. Finally, after changing a direction of an evolution at one of classical turning points, a probability current ends its evolution in the asymptotic region ($R \to \infty$) in one of the open scattering channels. Take note that a probability current evolution in an adiabatic molecular state $j$ occurs with a corresponding effective adiabatic potential $U_j^{\rm eff}$,

$$U_j^{\rm eff}(R, J) = U_j(R) + \frac{J(J+1)\hbar^2}{2\mu R^2}, \tag{3}$$

where $U_j(R)$ is an eigenvalue of the electronic Hamiltonian, that is, an adiabatic potential energy of the adiabatic state $j$, $J$ is a total angular momentum quantum number; $\mu$ is a reduced nuclear mass. This procedure is repeated $N_{\rm tot}$ times, and averaged populations of each scattering channel are determined. A single probability current has a weight $1/N_{\rm tot}$, all currents give a distribution of populations among all open final channels. The populations in the final channels yield the inelastic state-to-state probabilities for each transition from a given initial scattering channel $i$ to each open final scattering channel $f$, that is, the inelastic probabilities $P_{if}$ for each state-to-state transition $i \to f$. As soon as all inelastic probabilities $P_{if}(E, J)$ are known for each $J$ and each collision energy $E$ of interest, calculations of the inelastic partial cross sections $\sigma_{if}(E)$ and the partial rate coefficients $K_{if}(T)$ ($T$ being a temperature) for a transition $i \to f$ are straightforward,

$$\sigma_{if}(E) = \frac{\pi\hbar^2 p_i^{\rm stat}}{2\mu E}\sum_{J=0}^{\infty} P_{if}(E, J)(2J+1), \tag{4}$$

$$K_{if}(T) = \sqrt{\frac{8}{\pi\mu(k_B T)^3}}\int_0^{\infty} E\sigma_{if}(E)\exp\left(-\frac{E}{k_B T}\right)dE, \tag{5}$$

$p_i^{\rm stat}$ being the statistical probability for population of the initial channel $i$, $k_B$ the Boltzmann constant. Rate coefficients $K_{kn}(T)$ for exothermic processes $k \to n$ (we consider $E_k > E_n$) depend weakly on a temperature $T$, so they are calculated first, whereas the rate coefficients $K_{nk}(T)$ for endothermic processes $n \to k$ are then calculated via the detailed balance relation,

$$K_{nk}(T) = K_{kn}(T)\frac{p_n^{\rm stat}}{p_k^{\rm stat}}\exp\left(-\frac{\Delta E_{kn}}{k_B T}\right), \tag{6}$$

where $\Delta E_{kn} = E_k - E_n$ is the energy defect.

[2]Reference [27] does not provide enough information for using the reprojection method.

In the present paper, the total repeating number $N_{\rm tot} = 2621\,440\,000 = 2.621\,44 \times 10^9$, so the accuracy of the present calculation is significantly higher as compared with the previous calculation [28] where the repeating number was equal to 163 840. The uncertainty of the nonadiabatic transition probabilities in the present calculation is $3.8 \times 10^{-10}$ (a weight of a single probability current $1/N_{\rm tot}$ and, hence, the minimum transition probability, which can be accounted by the hopping probability current method for a given $N_{\rm tot}$), and it reaches the level of accuracy of full quantum calculations.

The main advantage of the probability current method used in the present calculations is that the method takes into account all nonadiabatic regions, long and short ranges, not only long-range regions located in a particular order and treated within asymptotic approaches, although in some cases it is sufficient to account only long-range regions, see Ref. [35].

It should be mentioned that for the deexcitation processes $^6\mathrm{Li}(2p)/\,^7\mathrm{Li}(2p) + \mathrm{H/D} \rightarrow {}^6\mathrm{Li}(2s)/^7\mathrm{Li}(2s) + \mathrm{H/D}$ corresponding to the resonance lines 670.776/670.791 nm, the deterministic version of the probability current method [35], the so-called branching probability current method, was used at low collisional energies. The reason is that the nonadiabatic transition probabilities between the ground and the first excited molecular states at collisional energies below 1 eV are so low that even $N_{\rm tot} = 2.62 \times 10^9$ probability currents in the hopping probability current method are insufficient for calculations of the total state-to-state probabilities. The branching probability current method can handle such low nonadiabatic transition probabilities, otherwise, the hopping probability current method works perfectly well. It is worth mentioning that although the inelastic state-to-state probability for the transition $\mathrm{Li}(2p \rightarrow 2s)$ in collisions with hydrogen is very low, nevertheless, it is important to know the rate coefficients for these transitions as accurate as possible because NLTE modeling of lithium spectrum in stellar atmospheres are using these resonance lines for determining lithium abundances.

Thus, the combination of the accurate *ab initio* electronic structure calculations [27] and the accurate nuclear dynamical calculations performed in the present paper yields the accurate cross sections and rate coefficients for the inelastic processes in lithium-hydrogen collisions for different isotopes.

## III. $^6$Li / $^7$Li +H/D/T COLLISIONS

In the present paper, the isotopic effects on all partial inelastic processes of mutual neutralization, ion-pair formation, excitation, and deexcitation in lithium-hydrogen collisions are considered for different isotopes of both collisional partners, namely, in collisions $\mathrm{z}^6\mathrm{Li} + \mathrm{H}$, $^6\mathrm{Li} + \mathrm{D}$, $^6\mathrm{Li} + \mathrm{T}$, $^7\mathrm{Li} + \mathrm{H}$, $^7\mathrm{Li} + \mathrm{D}$, and $^7\mathrm{Li} + \mathrm{T}$ as well as in collisions of the corresponding positive and negative ions. Let us first compare the results of the present calculations with the recent experimental data [21,24] and the recent calculations by other authors [21,27].

The present paper is performed by making use of the accurate *ab initio* electronic structure calculations [27] for seven covalent and one ionic molecular states shown in Table I. The analysis of the calculated potentials and couplings presented in the paper by Croft *et al.* [27] as well as the data collected in Table II and discussed above allow us to estimate the potential-energy error to be equal to $10^{-3}$ eV and, hence, to treat nonadiabatic nuclear dynamics accounting not only for the long-range, but also for the short-range regions. The probability current method, which accounts for both long- and short-range nonadiabatic regions, was chosen for this purpose.

For the treated inelastic processes the rate coefficients are computed in the temperature range of 1000–10 000 K. The calculated rate coefficients are available online as the Supplemental Material [52] to the present paper. The examples of the calculated rate coefficients, that is, the rates for $T = 6000$ K, are shown in the Appendix. For computing the rates, the cross sections are calculated in the collision energy range of 0.001–100 eV. Concerning the quantum number $J$ in the sum (4) for computing the cross sections, the upper summation limit $J_{\rm max}$ depends on the collision energy $E$, and it is determined as a value of the total angular momentum quantum number exceeding which all inelastic state-to-state transition probabilities are equal to zero.

The main isotopic effects appear due to nonadiabatic nuclear dynamics, that is, due to the motion of particles with different nuclear reduced masses of the collisional partners. Two main effects [from here and on noted as (I) and (II)] occur in nuclear dynamical calculations: (I) At a given collision energy $E_{\rm col}$, the radial velocity $v$ at the center of a nonadiabatic region depends on the reduced nuclear mass $\mu$ of the system. At a fixed value of the Landau-Zener parameter $\xi$, the Landau-Zener transition probability (1) is lower for heavier colliding partners, and a cross section decreases; it should be pointed out that this effect is stronger at low collisional energies (lower than 1 eV) than at high energies. (II) On the other hand, increasing a reduced nuclear mass leads to slower growing of the effective potential-energy Eq. (3) as a function of the total angular momentum quantum number $J$. So, the upper limit in sum (4) is greater for heavier colliding partners, and a cross section increases. Thus, there are two opposite isotopic effects, and results of their influence on partial cross sections are not uniquely defined.

In general, two cases should be considered in lithium-hydrogen collisions: (i) isotopic effects due to the lithium isotopes $^6$Li and $^7$Li in collisions with hydrogen, and (ii) isotopic effects due to the hydrogen isotopes, that is, hydrogen, deuterium, and tritium, in collisions with lithium. We analyze both effects below.

Before discussing the isotopic effects, let us briefly mention the main features of the inelastic processes in lithium-hydrogen ($\mathrm{Li} + \mathrm{H}$ and $\mathrm{Li}^+ + \mathrm{H}^-$) collisions. The details of these features and the comparison with other available data, but isotopic effects are described in Ref. [28].

The first feature is that the mutual neutralization processes are dominant over other inelastic processes. The second one is that among the partial mutual neutralization processes, the largest values of the cross sections and rate coefficients correspond to the process with the final channel $\mathrm{Li}(3s) + \mathrm{H}$ and then the next processes with the final channels $\mathrm{Li}(3p, 3d) + \mathrm{H}$. The rates of the mutual neutralization processes depend on a single binding energy of the final channel with the maximum rate at the binding energy roughly equals $-2$ eV. For the excitation and deexcitation processes, the rate coefficients depend on two binding energies of the initial and the final

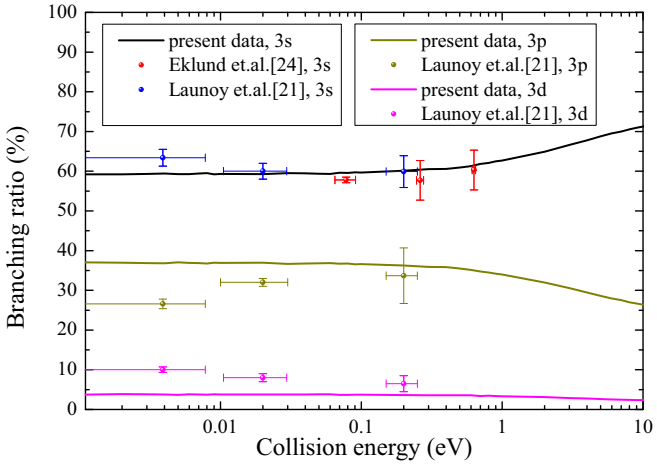


FIG. 1. Branching ratio of the cross sections for the partial mutual neutralization processes $^7Li^+ + D^- \to {}^7Li(3s, 3p, 3d) + D$ to the total cross section for the neutralization processes $^7Li^+ + D^- \to {}^7Li(3s, 3p, 3d) + D$ as a function of the collision energy. Solid line corresponds to the present calculation, red circles correspond to the experimental data of Ref. [24], blue, magenta, and dark yellow circles correspond to the experimental data of Ref. [21].

channels with the maximum values of the binding energies approximately equal also −2 eV. The maximum values of the rate coefficients for excitation and deexcitation processes are roughly by an order of magnitude smaller than that for the mutual neutralization processes. Outside of these regions with the maximal values of rate coefficients[3] the rates get lower values. The reaction mechanism of the partial processes with the highest and moderate rates mainly correspond to the long-range ionic-covalent interactions, whereas for the processes with low rates the mechanisms are both the ionic-covalent and the short-range "loop" ones.

Let us turn to the comparison of the present lithium-hydrogen-collision data with the previous recent experimental and theoretical data [21,24,27]. It is worth noting that the experimental data [24] consist of three signals corresponding to the mutual neutralization processes $^7Li^+ + D^- \to {}^7Li(3s, 3p, 3d) + D$. One of the signals, $^7Li^+ + D^- \to {}^7Li(3s) + D$ is well separated, whereas two others, $^7Li^+ + D^- \to {}^7Li(3p, 3d) + D$, are not distinguishable. The experimental data [21] consist of three distinguishable signals, $^7Li^+ + D^- \to {}^7Li(3s, 3p, 3d) + D$. No other signals were observed. The present calculation shows that the signals for other partial processes are too weak to be detected in agreement with the experimental observations. All experimental signals were measured in relative units, so in order to have them in absolute units, e.g., in Å$^2$, one needs to have a reference point. Such a reference point could be a calculated cross section, for instance, for the partial process with the highest cross section $^7Li^+/{}^6Li^+ + H^-/D^- \to {}^7Li/{}^6Li(3s) + H/D$.

Figure 1 depicts the branching ratios of the recent experimental data [21,24], the recent calculation [21], and the present calculation. The good agreement of the experimental [21,24] and the present theoretical data is seen for all three processes $^7Li^+ + D^- \to {}^7Li(3s, 3p, 3d) + D$ in the collision energy range of 0.05–1 eV. The recent measurements [21,24] do not provide data for collision energies higher than this range. For collision energies $E_{col}$ lower this range, the present calculation yields nearly constant branching ratios with decreasing $E_{col}$, whereas the experimental data demonstrate the slow increase branching ratios for the $(3s)$ and $(3d)$ states or the decrease for the $(3p)$ state [21]. According to the definition of a cross-section $\sigma_{if}(E_{col})$ Eq. (4) a cross section at the zero-energy limit behaves as follows: $\sigma_{if}(E_{col}) = \text{const}/E_{col}$ where const is an individual constant for each partial process; see also Ref. [21] for the similar energy dependence. Such energy dependence for all partial processes leads to constant branching ratios as a function of $E_{col}$. The matter of the fact is that decreasing or increasing an absolute value of one partial cross section can result in increasing or decreasing branching ratios for other cross sections though their absolute values are kept unchanged. Thus, the increasing or decreasing branching ratio at decreasing collision energy does not necessary mean increasing or decreasing const values.[4].

Launoy *et al.* [21] also reported a theoretical study of the mutual neutralization processes in $^7Li^+ + D^-$ collisions. That study was based on the *ab initio* electronic structure calculation (potentials and NACMEs) with augmented basis functions located at different positions.[5] They treated the nuclear dynamics by means of the multichannel LZ approach in which only long-range nonadiabatic regions created by the ionic-covalent interaction were taken into account, although the *ab initio* calculations indicate on the existence of short-range nonadiabatic regions as well. The LZ parameters, including locations of nonadiabatic regions, were determined from calculated maximal values of NACMEs, which are, in turn, determined by the augmented basis functions and their locations. The augmented functions and their locations were adjusted by Launoy *et al.* [21] in such a way that the calculated branching ratios for the mutual neutralization processes in $^7Li^+ + D^-$ collisions to agree with the measured ones. Finally, Launoy *et al.* [21] found the augmented functions and their locations which provide branching ratios in the best agreement with the experimental data, the accuracy was found within $\approx \pm(3–5)\%$. We estimate our present results to be within $\approx \pm(5–10)\%$ with both experimental and theoretical data [21,24]. We treat this as good agreement and assume the same accuracy for other processes in lithium-hydrogen collisions, in particular, for the excitation and deexcitation ones. However, some discrepancies between theoretical and

[3]These regions are called the optimal windows for inelastic processes in collisions with hydrogen.

[4]The energy dependence of a cross-section $\sigma_{if}(E) = \text{const}/E$ has a singularity at the zero-energy point. In the very limit, every constant const in the cross-section $\sigma_{if}(E)$ Eq. (4) is determined by the only partial wave with $J = 0$, although at low but not zero energy each const is determined by several partial waves with the quantum wave numbers $J = 0, J_{max}$, but const are still constants with high accuracy

[5]Note that NACME depends on a location of an electron origin. Although it is not stated exactly in Ref. [21], we assume that in that paper the electron origin was put in the center of nuclear mass as it should be, see Ref. [40].

experimental data still exist, and this warrants further experimental and theoretical investigations, perhaps by means of the inclusion of other reaction mechanisms or performing full quantum calculations and/or additional measurements.

It is worth emphasizing that some rate coefficients computed in the present paper deviate in both directions from the values published in Ref. [28]. For example, at $T = 6000$ K the largest rates for the mutual neutralization processes with the final channels $\mathrm{Li}(3s, 3p, 3d) + \mathrm{H}$ were equal to $9.47 \times 10^{-8}$, $4.00 \times 10^{-8}$, and $3.71 \times 10^{-9}$ cm$^3$/s, respectively, [28], whereas the present calculation yields $8.50 \times 10^{-8}$, $3.74 \times 10^{-8}$, and $3.53 \times 10^{-9}$ cm$^3$/s, that is, 11, 7, and 5% smaller. On the other hand, the new rate coefficient for the mutual neutralization with the final channel $\mathrm{Li}(4s) + \mathrm{H}$ at $T = 6000$ K is larger than the old one by 32%, that is, $2.31 \times 10^{-10}$ cm$^3$/s (old) vs $3.05 \times 10^{-10}$ cm$^3$/s (new). All these changes occur due to an increase in the total number of probability currents by four orders of magnitude, which increases the accuracy substantially as well as due to the increase in the reduced nuclear mass in the present calculation. Changing rate coefficient values with the changing of probability currents number affects not only mutual neutralization, but other process rates as well, in particular, excitation and deexcitation ones. For instance, the new rate for the resonance transition process $^7\mathrm{Li}(2p \to 2s) + \mathrm{H}$ at $T = 6000$ K is smaller by a factor of 38 than the old rate, that is, $6.53 \times 10^{-14}$ cm$^3$/s (old) vs $1.71 \times 10^{-15}$ cm$^3$/s (new). Obviously, the larger rate coefficient the less dependent its value on a probability current number used in calculation, although this rule is approximate.

Concerning the isotopic effect, Launoy *et al.* [21] wrote that they also obtained the experimental branching ratios for $\mathrm{Li}^+ + \mathrm{H}^-$ collisions, and these values are similar to those measured for $\mathrm{Li}^+ + \mathrm{D}^-$. Finally, they concluded: "We observed no clear isotope effect."

### A. Lithium isotopic effects

Let us discuss the effects due to participation of different lithium isotopes in lithium-hydrogen collisions. In the present paper, the inelastic processes for all transitions between the scattering channels collected in Table I are calculated for all possible isotopic pairs, and the isotopic effects are analyzed. Since the mutual neutralization processes are of particular importance, the cross sections for these processes are shown in Figs. 2 and 3 for different isotopes. It is seen from these figures that the isotopic effects due to participation of different lithium isotopes in $^{6,7}\mathrm{Li} + \mathrm{H/D/T}$ collisions are marginal for the majority of the processes.[6] At high collision energies, the difference between cross sections in collisions of hydrogen with different lithium isotopes is negligible. For example, the cross sections for the process $^{6,7}\mathrm{Li}(2p) + \mathrm{H} \to {}^{6,7}\mathrm{Li}(2s) + \mathrm{H}$ at energy Ecol = 100 eV are $\sigma_{21}^{^6\mathrm{Li\,H}} = 0.256\,1464$ Å$^2$ and $\sigma_{21}^{^7\mathrm{Li\,H}} = 0.250\,8187$ Å$^2$, and the difference is $\approx 2\%$.[7] On the other hand, the same process at $E_{\mathrm{col}} =$ 0.1 eV has the cross-sections $\sigma_{21}^{^6\mathrm{Li\,H}} = 2.748\,31 \times 10^{-7}$ Å$^2$, $\sigma_{21}^{^7\mathrm{Li\,H}} = 2.26535 \times 10^{-7}$ Å$^2$, and the difference $\approx 20\%$.

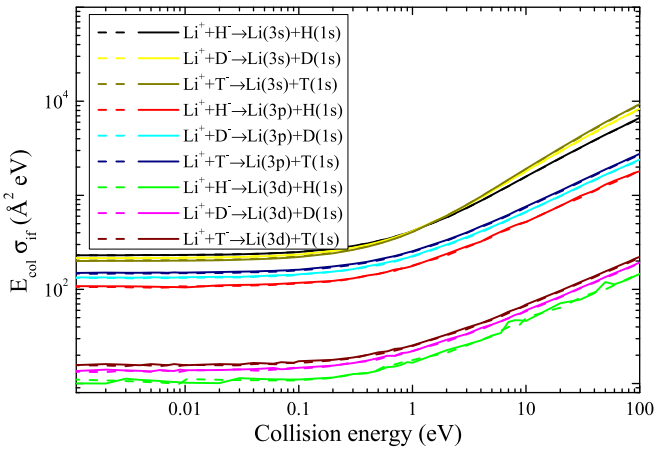


FIG. 2. Cross sections $\sigma_{if}$ (in the units of Å$^2$ multiplied by the collision energy $E_{\mathrm{col}}$ (in the units of eV) for the mutual neutralization processes in collisions of various isotopes of $\mathrm{Li}^+ + \mathrm{H}^-$. Solid lines correspond to $^7\mathrm{Li}^+ + \mathrm{H}^-/\mathrm{D}^-/\mathrm{T}^-$ collisions, and dashed lines correspond to to $^6\mathrm{Li}^+ + \mathrm{H}^-/\mathrm{D}^-/\mathrm{T}^-$ collisions.

For all processes, a difference between cross sections for $^6\mathrm{Li}\,/\,^7\mathrm{Li} + \mathrm{H}$ and $^6\mathrm{Li}\,/\,^7\mathrm{Li} + \mathrm{D}$ is varying from 1–3% to 25–40%. At low collision energies ($< 1.0$ eV), the difference is typically larger than at higher collision energy. A small difference can be explained by the fact that in this case the reduced masses $\mu$ (in atomic unit of mass, a.u.m.) are close to each other:

(1) $\mu^{^6\mathrm{Li\,H}} = 0.863\,197$, $\mu^{^7\mathrm{Li\,H}} = 0.881\,238$;
(2) $\mu^{^6\mathrm{Li\,D}} = 1.508\,872$, $\mu^{^7\mathrm{Li\,D}} = 1.56\,4870$;
(3) $\mu_{^6\mathrm{Li\,T}} = 2.008\,810$, $\mu^{^7\mathrm{Li\,T}} = 2.109\,300$.

One can see from Figs. 2 and 3, that the cross sections for the mutual neutralization processes with participation of the lithium isotope $^6$Li are slightly larger than the cross sections with the isotopes $^7$Li, or there is no difference at all. Thus, the first conclusion is that for the mutual neutralization processes the influence of the isotopic effect (I) is stronger than the effect (II).

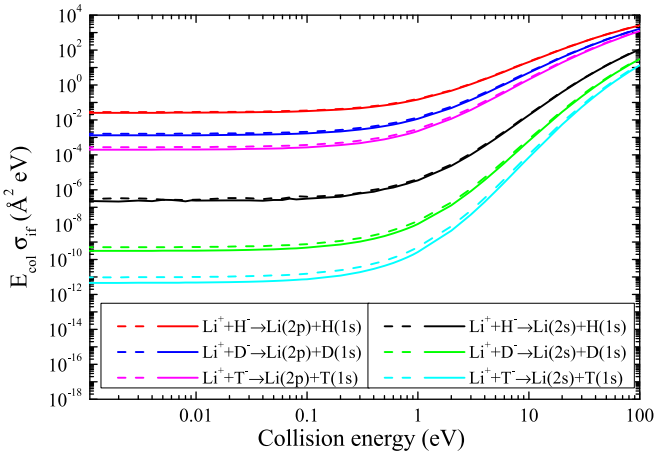


FIG. 3. The same as in Fig. 2 but for low-lying final channels: $f = 1, 2$.

[6]Note that the solid lines correspond to participation of the isotopes $^7$Li, whereas the dashed lines correspond to $^6$Li.

[7]Low indices show an initial $i$ and a final $f$ channel and, hence, the transition $i \to f$, see Table I.

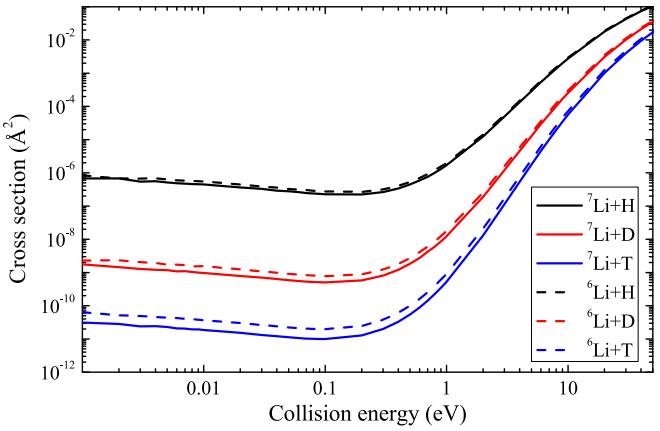


FIG. 4. The partial cross sections corresponding to the deexcitation process $\mathrm{Li}(2p) + \mathrm{H} \to \mathrm{Li}(2s) + \mathrm{H}$. The black solid line corresponds to the process in $^7$Li +H collisions, the black dashed line corresponds to the process in $^6$Li +H collisions, the red solid line corresponds to the process in $^7$Li +D collisions, the red dashed line corresponds to the process in $^6$Li +D, blue solid line corresponds to the process in $^7$Li +T, and the blue dashed line corresponds to the process in $^6$Li +T.

It is worth emphasizing that Figs. 2 and 3 present the mutual neutralization cross sections multiplied by the collision energy, and these products go to constant values at low-collision energies. This confirms that at the zero-collision-energy limit only the $s$ partial wave contributes into the cross section as it should be in according to Eq. (4). Finally, this leads to the following collision-energy dependence of the mutual neutralization cross section $\sigma_{if}(E_{\mathrm{col}}) = \mathrm{const}/E_{\mathrm{col}}$. As mentioned above, this energy dependence results in constant branching ratios at the collision energy goes to zero. This is what is observed experimentally in Refs. [21,24], see also Fig. 1.

### B. Hydrogen isotopic effects

Let us first discuss hydrogen isotopic effects for the processes with participation of the ground and the first excited states of lithium. For the processes in $^6$Li +H/D/T and $^7$Li +H/D/T collisions with participation of the ground-state $\mathrm{Li}(2s) + \mathrm{H/D/T}$ and the first excited-state $\mathrm{Li}(2p) + \mathrm{H/D/T}$ the isotopic effects are most significant, see Figs. 3 and 4. For these processes the difference between the cross sections in $^6$Li +H/D/T and $^7$Li +H/D/T collisions may exceed two orders of magnitude. For example, at collision energy $E_{\mathrm{col}} = 0.01$ eV the cross sections for the resonant deexcitation process $^7\mathrm{Li}(2p) + \mathrm{H/D} \to {}^7\mathrm{Li}(2s) + \mathrm{H/D}$ are $\sigma_{21}^{^7\mathrm{Li\,H}} = 4.505\,31 \times 10^{-7}$ and $\sigma_{21}^{^7\mathrm{Li\,D}} = 9.692\,28 \times 10^{-10}$ Å$^2$, that is, replacing H by D at $E_{\mathrm{col}} = 0.01$ eV decreases the resonant deexcitation cross section by a factor of 465.

Comparing the present cross sections with the previously calculated data, one can note that the great difference between the cross sections can be explained by the significant difference in the reduced masses, almost up to a factor of 2:

(1) $\mu^{^6\mathrm{Li\,H}} = 0.863\,197$, $\mu^{^6\mathrm{Li\,D}} = 1.508\,872$, $\mu^{^6\mathrm{Li\,T}} = 2.008\,810$;

(2) $\mu^{^7\mathrm{Li\,H}} = 0.881\,238$, $\mu^{^7\mathrm{Li\,D}} = 1.564\,870$, $\mu^{^7\mathrm{Li\,T}} = 2.109\,300$,

where the reduced masses are written in units of a.u.m. In this case, both effects influence differently for different processes. For the processes with participation of the ground and the first excited states, the cross sections for $^6$Li / $^7$Li +D are significantly lower than for $^6$Li / $^7$Li +H, more than one order of magnitude. So, one can conclude that in this case the effect (I) is stronger than the effect (II). On the other hand, for processes with participation of the states 3–7 and ionic (see Table I) the cross sections are slightly greater in collisions $^6$Li / $^7$Li +D than in $^6$Li / $^7$Li +H. It can be concluded that for these processes the effect (II) is stronger than the effect (I).

### C. Rate coefficients

Let us now discuss the calculated rate coefficients for the processes in lithium-hydrogen collisions. The rate coefficients for all considered inelastic processes in lithium-hydrogen collisions are calculated for the temperature range of 1000–10 000 K. The rates for the mutual neutralization processes into the final-states $\mathrm{Li}(3l)$ at temperatures of $T = 6000$ K are collected in Table III. This table also shows the comparison of the data, calculated in the present paper with ones measured by Launoy *et al.* [21] for the states $\mathrm{Li}(3s)$, $\mathrm{Li}(3p)$, $\mathrm{Li}(3d)$, see also Fig. 1. One can see that the rates for the mutual neutralization processes into the final scattering channels $\mathrm{Li}(3l) + \mathrm{H}$, calculated in the present paper are in good agreement with the experimental data [21,24]. It is also seen that the present total rate coefficient is in a good agreement with one computed by Croft *et al.* [26].[8] Both calcula-

[8]Unfortunately, it is not possible to compare with the partial rates from Ref. [26].

TABLE III. Rate coefficients (in units of cm$^3$/s) of the mutual neutralization processes into the final-states $\mathrm{Li}(3l)$ at temperatures of $T = 6000$ K calculated in the present paper, measured in Ref. [21] and computed in Ref. [26] (from Fig. 2). Numerals in square brackets represent the power of 10.

| | | $3s$ | $3p$ | $3d$ | Total |
|---|---|---|---|---|---|
| Present calculation | $^7\mathrm{Li}^+ + \mathrm{H}^-$ | 8.50[−8] | 3.74[−8] | 3.53[−9] | 1.26[−7] |
| | $^7\mathrm{Li}^+ + \mathrm{D}^-$ | 6.30[−8] | 3.54[−8] | 3.51[−9] | 1.02[−7] |
| | $^6\mathrm{Li}^+ + \mathrm{H}^-$ | 8.59[−8] | 3.74[−8] | 3.60[−9] | 1.27[−7] |
| | $^6\mathrm{Li}^+ + \mathrm{D}^-$ | 6.43[−8] | 3.54[−8] | 3.49[−9] | 1.04[−7] |
| Experiment [21] | $^7\mathrm{Li}^+ + \mathrm{H}^-$ | 7.43[−8] | 2.72[−8] | 7.72[−9] | 1.10[−7] |
| | $^7\mathrm{Li}^+ + \mathrm{D}^-$ | 5.54[−8] | 2.57[−8] | 7.48[−9] | 8.90[−8] |
| Croft *et al.* [26] | $^7\mathrm{Li}^+ + \mathrm{H}^-$ | | | | 1.18[−7] |

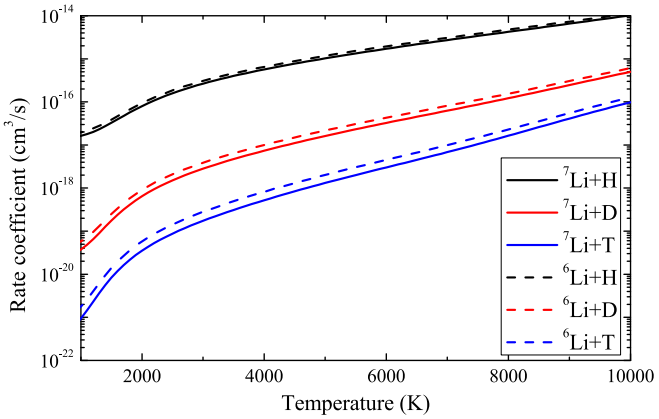


FIG. 5. The rate coefficients for the processes $^{6,7}\mathrm{Li}(2p) + \mathrm{H/D/T} \rightarrow {}^{6,7}\mathrm{Li}(2s) + \mathrm{H/D/T}$ as a function of the temperature for the range of 1000–10 000 K. Black solid line corresponds to $^7$Li +H collisions, red solid line corresponds to $^7$Li +D collisions, blue solid line corresponds to $^7$Li +T collisions, and dashed lines correspond to $^6$Li +H/D/T collisions, respectively.

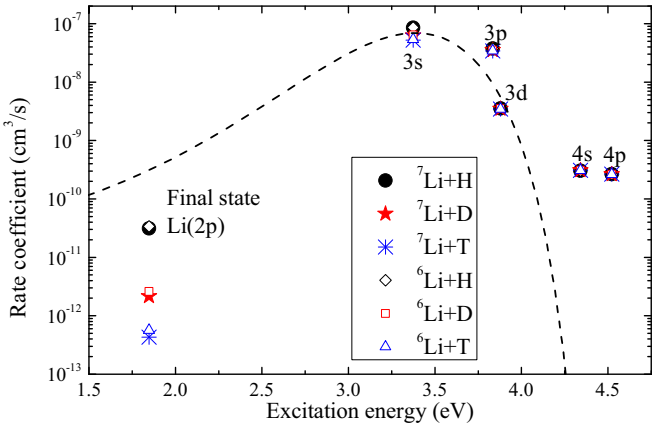


FIG. 6. The rate coefficients for the mutual neutralization processes $^{6,7}\mathrm{Li}^+ + \mathrm{H}^-/\mathrm{D}^-/\mathrm{T}^- \rightarrow {}^{6,7}\mathrm{Li} + \mathrm{H/D/T}$ as functions of the excitation energies of the final channels at temperatures of $T = 6000$ K. The symbols correspond to different collisional partners, see the figure for the labels. The dashed line depicts the estimate according to the simplified model.

tions, the present one and one by Croft *et al.* [26], indicate that the maximal cross section and the maximal rate coefficient correspond to the partial process of the mutual neutralization with the $\mathrm{Li}(3s) + \mathrm{H}$ final channel. The second maximal cross section and rate coefficient correspond to the mutual neutralization process into the $\mathrm{Li}(3p) + \mathrm{H}$ final channel.

The rate coefficients for the deexcitation processes $^{6,7}\mathrm{Li}(2p) + \mathrm{H/D} \rightarrow {}^{6,7}\mathrm{Li}(2s) + \mathrm{H/D}$, related to the resonance lines 670.776/670.791 nm, have low values. Figure 5 shows the temperature dependences of the rate coefficients for these processes. One can see that the rate coefficients for these processes have values lower than $10^{-15}$ cm$^3$ s$^{-1}$ at low temperatures ($T < 5000$ K), and only at temperatures higher than 10 000-K the rate coefficients exceed the value of $10^{-14}$ cm$^3$ s$^{-1}$ for the processes in collisions with H. The rate coefficients of the processes in collisions with deuterium have values of, at least, one order of magnitude lower than those in collisions with H, see Fig. 5.

The isotopic effects for these processes are the following. At temperature $T = 1000$ K the rate coefficients of the processes in $^6$Li +H collisions are ≈20% higher than the rates in $^7$Li +H collisions with the difference decreasing to ≈11% at 10 000 K. Concerning the collisions of $^{6,7}$Li with D, the similar behavior is hold, but the difference goes from ≈49% at $T = 1000$ K down to ≈22% at 10 000 K.

The isotopic effects are clearly seen in Fig. 6 where the rate coefficients for the mutual neutralization processes are plotted as functions of the excitation energy of the final lithium state at temperatures of $T = 6000$ K. Similar plots are depicted in Fig. 7, but for the excitation and deexcitation processes for the initial scattering channel $\mathrm{Li}(3s) + \mathrm{H}$. One can see in both figures that: (i) the isotopic effects is greater for participation of different hydrogen isotopes than lithium isotopes; (ii) the isotopic effects are larger for low-lying states than for high-lying ones.

All calculated rate coefficients for the inelastic processes in $^6$Li +H, $^6$Li +D, $^6$Li +T, $^7$Li +H, $^7$Li +D, and $^7$Li +T collisions are tabulated for temperatures from 1000 to 10 000 K with the step 1000 K and available as the Supplemental Material [52]. The examples of the calculated rate coefficients are given in the Appendix for the temperature $T = 6000$ K.

## IV. CONCLUSION

In the present paper, the inelastic processes in lithium-hydrogen collisions are studied, in particular, for different isotopes of both lithium and hydrogen. The following processes are investigated: Mutual neutralization in collisions of the corresponding positive and negative ions $^6$Li$^+$ +H$^-$, $^6$Li$^+$ +D$^-$, $^6$Li$^+$ +T$^-$, $^7$Li$^+$ +H$^-$, $^7$Li$^+$ +D$^-$, and $^7$Li$^+$ +T$^-$ as well as the processes of ion-pair formation, excitation, and deexcitation in collisions

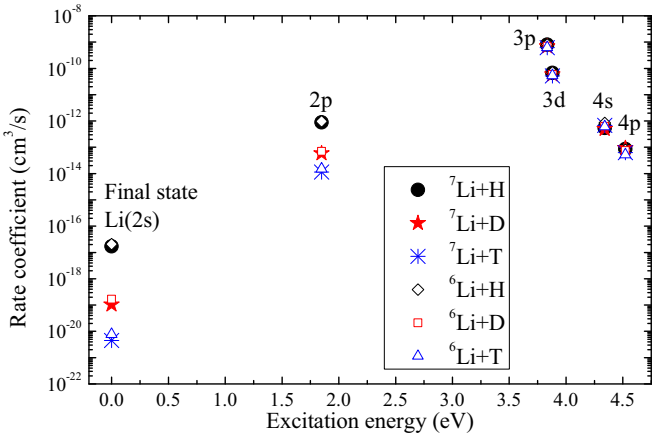


FIG. 7. The rate coefficients for the excitation and deexcitation processes from the initial channels $^{6,7}\mathrm{Li}(3s) + \mathrm{H/D/T}$ as functions of the excitation energies of the final channels at the temperatures of $T = 6000$ K. The symbols correspond to different collisional partners, see the figure for the labels.

$^6$Li +H, $^6$Li +D, $^6$Li +T, $^7$Li +H, $^7$Li +D, and $^7$Li +T. Fifty-six partial inelastic processes in total are treated. The paper is performed by making use of seven covalent and one ionic molecular states for which the *ab initio* electronic structure has been calculated by Croft *et al.* [27]. The nonadiabatic nuclear dynamics is treated by means of the hopping probability current method (the probabilistic version of the probability current method) [28,35,45]. In addition, the branching probability current method (the deterministic version of the probability current method) [35] was used for treating the deexcitation processes $^{6,7}\mathrm{Li}(2p \rightarrow 2s) + \mathrm{H/D/T}$ corresponding to the resonance lines. The hopping probability current method requires to repeat calculations of probability current evolution at each given set of initial collisional parameters. In the present paper, this repeating number of the currents is equal to $N_{\mathrm{tot}} = 2.621\,44 \times 10^9$. This huge number of the repeated probability currents provides high accuracy in the calculations of the state-to-state transition probabilities, roughly $2 \times 10^{-5}$, and the minimal transition probability being equal to $3.8 \times 10^{-10}$. This accuracy exceeds the accuracy of the previous quantum calculations, see Ref. [28] and references therein. So, the first result of the present paper is the rate coefficients for the different inelastic processes in lithium-hydrogen collisions calculated with the highest up to now accuracy for various isotopes of both lithium and hydrogen.

The rate coefficients for the treated inelastic processes are calculated for the temperature range of 1000–10 000 K. The computed rate coefficients are available online as the Supplemental Material [52] to the present paper. As the example, the rate coefficients for $T = 6000$ K are shown in the Appendix.

The comparison of the calculated data with the available recent experimental results [21,24] as well as with the previously computed quantum total rate for the mutual neutralization [27] shows good agreement. It is worth mentioning that the recent experimental data [21,24] are available only for the very limited number of states: Li($3s$, $3p$, $3d$) for a very limited range of a collision energy and only for the mutual neutralization processes. Within these limits, the isotopic effects look to be moderate. However, it is found in the present paper that for some cases the isotopic effects can be strong, whereas in other cases the effects are rather weak, see below for particular findings. These findings were revealed due to the present accurate dynamical calculations performed for all partial processes between the considered states and for a rather wide range of collision parameters, including accounting for short-range nonadiabatic regions in addition to the long-range ones due to the ionic-covalent interaction.

Analysis of the calculated rate coefficients shows that the isotopic effects are greater for hydrogen isotopes than for lithium ones. The isotopic effects on lithium are marginal: Replacing $^6$Li by $^7$Li changes a cross section or a rate coefficient by a few percents only.

The next finding is the following. The larger value of a cross section or a rate coefficient the weaker isotopic effect on replacing a hydrogen atom by another isotope in its collisions with a lithium atom in a low-lying states. Actually, this means that an isotopic effect depends on an excitation energy (or a binding energy) of the state(s) considered. If an asymptotic energy of an initial or a final scattering channel belongs to an optimal window, then an inelastic cross section and a corresponding rate coefficient have maximal values and a hydrogen isotopic effect is weak. In particular, for the Li($3s$, $3p$, $3d$) states, the hydrogen isotopic effects are from 1 to 50%. For the higher-lying lithium states, the hydrogen isotopic effects are practically negligible. For low-lying lithium states, in particular, for the ground and the first excited lithium states, the isotopic effects are the greatest. For example, changing a hydrogen isotope in its collisions with a lithium atom in the ground or the first-excited states could lead to changing of partial cross sections and partial rate coefficients up to several orders of magnitude.

The present accurate calculations allowed us to investigate the hydrogen isotopic effect on the resonance process $\mathrm{Li}(2p) + \mathrm{H/D/T} \rightarrow \mathrm{Li}(2s) + \mathrm{H/D/T}$, which is important for astrophysical NLTE modeling. It is found that the hydrogen isotopic effect for this process is the strongest. For example, at the temperature of $T = 6000$ K, the rate coefficients for the process in collisions $^7\mathrm{Li} + \mathrm{H/D/T}$ are equal to $1.71 \times 10^{-15}$, $3.26 \times 10^{-17}$, and $3.02 \times 10^{-18}$ cm$^3$/s, respectively.

Generalizing these findings, the following rule can be formulated: The hydrogen isotopic effects are negligible when a Massey parameter (or the Landau-Zener parameter divided by a radial velocity at a center of a main nonadiabatic region) is small (a highly excited interacting states, a long-range region); the effects are weak when a Massey parameter is close to unit, and the hydrogen isotopic effects are strong when a Massey parameter is large.

Thus, in the present paper, the hydrogen isotopic effects have been studied for all states from the ground Li($2s$) to the high-excited one Li($4p$) and to the ionic state $\mathrm{Li}^+ + \mathrm{H}^-$. This allowed us to investigate the isotopic effects not only for the mutual neutralization processes, but also for the excitation, deexcitation, and ion-pair formation processes. It is found that the hydrogen isotopic effects are different for different hydrogen isotopes and for different states, in particular, the isotopic effect is stronger for T than for D.

## ACKNOWLEDGMENTS

We gratefully acknowledge support from the Ministry of Education (the Russian Federation), Project No. FSZN-2020-0026.

## APPENDIX: RATE COEFFICIENTS FOR DIFFERENT ISOTOPES IN LITHIUM-HYDROGEN COLLISIONS

Table IV shows the examples of the rate coefficients for all partial inelastic processes in lithium-hydrogen collisions for the different isotopes at temperature $T = 6000$ K. The partial processes treated are mutual neutralization, ion-pair formation, excitation, and deexcitation. The initial and the final scattering channels are listed in Table I. The lithium isotopes are $^6$Li and $^7$Li, whereas the hydrogen isotopes are H, D, and T. The complete set of the calculated rates is available online as a Supplemental Material [52] to the present paper [52].

TABLE IV. Rate coefficients (in units of $cm^3/s$) for all partial inelastic processes in lithium-hydrogen collisions for different isotopes at temperature $T = 6000$ K. Numerals in square brackets represent the power of 10.

| | | | | $^6$Li +H | | | | |
|---|---|---|---|---|---|---|---|---|
| | $2s$ | $2p$ | $3s$ | $3p$ | $3d$ | $4s$ | $4p$ | $Li^+ + H^-$ |
| $2s$ | | 1.64[−16] | 3.05[−20] | 2.30[−21] | 2.19[−22] | 3.16[−24] | 1.54[−24] | 5.58[−20] |
| $2p$ | 1.94[−15] | | 1.70[−14] | 1.79[−15] | 1.02[−16] | 2.01[−18] | 2.42[−19] | 1.28[−14] |
| $3s$ | 2.08[−17] | 9.75[−13] | | 8.08[−10] | 7.10[−11] | 8.35[−13] | 8.03[−14] | 1.86[−09] |
| $3p$ | 1.27[−18] | 8.36[−14] | 6.56[−10] | | 4.75[−11] | 3.35[−13] | 3.83[−14] | 6.59[−10] |
| $3d$ | 7.95[−20] | 3.10[−15] | 3.78[−11] | 3.11[−11] | | 1.27[−10] | 1.13[−11] | 4.15[−11] |
| $4s$ | 1.40[−20] | 7.51[−16] | 5.42[−12] | 2.68[−12] | 1.55[−09] | | 7.78[−11] | 4.29[−11] |
| $4p$ | 3.22[−21] | 4.26[−17] | 2.47[−13] | 1.45[−13] | 6.55[−11] | 3.68[−11] | | 1.76[−11] |
| $Li^+ + H^-$ | 1.76[−15] | 3.40[−11] | 8.59[−08] | 3.74[−08] | 3.60[−09] | 3.04[−10] | 2.64[−10] | |
| | | | | $^7$Li +H | | | | |
| | $2s$ | $2p$ | $3s$ | $3p$ | $3d$ | $4s$ | $4p$ | $Li^+ + H^-$ |
| $2s$ | | 1.44[−16] | 2.51[−20] | 1.87[−21] | 1.79[−22] | 5.49[−24] | 1.76[−24] | 4.70[−20] |
| $2p$ | 1.71[−15] | | 1.55[−14] | 1.63[−15] | 9.24[−17] | 1.83[−18] | 2.28[−19] | 1.18[−14] |
| $3s$ | 1.71[−17] | 8.91[−13] | | 8.03[−10] | 6.77[−11] | 5.46[−13] | 8.67[−14] | 1.84[−09] |
| $3p$ | 1.04[−18] | 7.61[−14] | 6.52[−10] | | 4.60[−11] | 2.84[−13] | 3.85[−14] | 6.59[−10] |
| $3d$ | 6.50[−20] | 2.82[−15] | 3.60[−11] | 3.01[−11] | | 1.26[−10] | 1.12[−11] | 4.08[−11] |
| $4s$ | 2.43[−20] | 6.82[−16] | 3.55[−12] | 2.28[−12] | 1.54[−09] | | 7.64[−11] | 4.30[−11] |
| $4p$ | 3.69[−21] | 4.02[−17] | 2.66[−13] | 1.46[−13] | 6.47[−11] | 3.61[−11] | | 1.78[−11] |
| $Li^+ + H^-$ | 1.48[−15] | 3.12[−11] | 8.50[−08] | 3.74[−08] | 3.53[−09] | 3.05[−10] | 2.66[−10] | |
| | | | | $^6$Li +D | | | | |
| | $2s$ | $2p$ | $3s$ | $3p$ | $3d$ | $4s$ | $4p$ | $Li^+ + H^-$ |
| $2s$ | | 3.66[−18] | 2.44[−22] | 3.26[−23] | 2.79[−24] | 2.06[−24] | 6.40[−25] | 3.67[−22] |
| $2p$ | 4.35[−17] | | 1.22[−15] | 1.16[−16] | 6.35[−18] | 1.19[−19] | 1.69[−20] | 9.87[−16] |
| $3s$ | 1.66[−19] | 7.01[−14] | | 6.92[−10] | 5.90[−11] | 6.27[−13] | 7.51[−14] | 1.40[−09] |
| $3p$ | 1.81[−20] | 5.40[−15] | 5.62[−10] | | 5.18[−11] | 3.99[−13] | 3.90[−14] | 6.23[−10] |
| $3d$ | 1.01[−21] | 1.94[−16] | 3.14[−11] | 3.40[−11] | | 1.05[−10] | 9.39[−12] | 4.03[−11] |
| $4s$ | 9.15[−21] | 4.43[−17] | 4.08[−12] | 3.20[−12] | 1.28[−09] | | 5.53[−11] | 4.45[−11] |
| $4p$ | 1.34[−21] | 2.99[−18] | 2.31[−13] | 1.48[−13] | 5.42[−11] | 2.61[−11] | | 1.77[−11] |
| $Li^+ + H^-$ | 1.15[−17] | 2.61[−12] | 6.43[−08] | 3.54[−08] | 3.49[−09] | 3.16[−10] | 2.65[−10] | |
| | | | | $^7$Li +D | | | | |
| | $2s$ | $2p$ | $3s$ | $3p$ | $3d$ | $4s$ | $4p$ | $Li^+ + H^-$ |
| $2s$ | | 2.74[−18] | 1.53[−22] | 1.67[−23] | 2.20[−24] | 2.94[−25] | 4.29[−25] | 2.51[−22] |
| $2p$ | 3.26[−17] | | 1.01[−15] | 9.51[−17] | 5.24[−18] | 9.65[−20] | 1.73[−20] | 8.19[−16] |
| $3s$ | 1.04[−19] | 5.82[−14] | | 6.84[−10] | 5.90[−11] | 4.94[−13] | 9.29[−14] | 1.37[−09] |
| $3p$ | 9.23[−21] | 4.43[−15] | 5.56[−10] | | 5.20[−11] | 5.70[−13] | 6.65[−14] | 6.23[−10] |
| $3d$ | 7.98[−22] | 1.60[−16] | 3.14[−11] | 3.41[−11] | | 1.04[−10] | 9.28[−12] | 4.05[−11] |
| $4s$ | 1.30[−21] | 3.60[−17] | 3.21[−12] | 4.57[−12] | 1.27[−09] | | 5.46[−11] | 4.37[−11] |
| $4p$ | 8.99[−22] | 3.06[−18] | 2.85[−13] | 2.51[−13] | 5.36[−11] | 2.58[−11] | | 1.75[−11] |
| $Li^+ + H^-$ | 7.89[−18] | 2.17[−12] | 6.30[−08] | 3.54[−08] | 3.51[−09] | 3.10[−10] | 2.63[−10] | |
| | | | | $^6$Li +T | | | | |
| | $2s$ | $2p$ | $3s$ | $3p$ | $3d$ | $4s$ | $4p$ | $Li^+ + H^-$ |
| $2s$ | | 3.80[−19] | 1.13[−23] | 7.29[−25] | 5.53[−26] | 7.01[−28] | 1.09[−28] | 1.86[−23] |
| $2p$ | 4.52[−18] | | 2.64[−16] | 2.32[−17] | 1.27[−18] | 2.42[−20] | 2.38[−21] | 2.14[−16] |
| $3s$ | 7.68[−21] | 1.51[−14] | | 6.26[−10] | 5.35[−11] | 6.10[−13] | 5.26[−14] | 1.17[−09] |
| $3p$ | 4.04[−22] | 1.08[−15] | 5.08[−10] | | 5.47[−11] | 4.74[−13] | 2.91[−14] | 6.04[−10] |
| $3d$ | 2.01[−23] | 3.89[−17] | 2.85[−11] | 3.58[−11] | | 9.51[−11] | 8.33[−12] | 4.00[−11] |
| $4s$ | 3.11[−24] | 9.03[−18] | 3.97[−12] | 3.80[−12] | 1.16[−09] | | 4.89[−11] | 4.34[−11] |
| $4p$ | 2.29[−25] | 4.19[−19] | 1.62[−13] | 1.10[−13] | 4.81[−11] | 2.31[−11] | | 1.76[−11] |
| $Li^+ + H^-$ | 5.86[−19] | 5.66[−13] | 5.40[−08] | 3.43[−08] | 3.47[−09] | 3.08[−10] | 2.64[−10] | |

TABLE IV. (*Continued.*)

| $^7$Li +T | | | | | | | | |
|---|---|---|---|---|---|---|---|---|
| | $2s$ | $2p$ | $3s$ | $3p$ | $3d$ | $4s$ | $4p$ | $Li^+ + H^-$ |
| $2s$ | | 2.54[−19] | 6.57[−24] | 3.80[−25] | 4.42[−26] | 3.63[−28] | 7.02[−29] | 1.09[−23] |
| $2p$ | 3.02[−18] | | 2.00[−16] | 1.74[−17] | 8.75[−19] | 1.20[−20] | 1.73[−21] | 1.62[−16] |
| $3s$ | 4.48[−21] | 1.15[−14] | | 6.13[−10] | 5.20[−11] | 6.86[−13] | 6.27[−14] | 1.14[−09] |
| $3p$ | 2.11[−22] | 8.11[−16] | 4.98[−10] | | 5.49[−11] | 3.83[−13] | 5.10[−14] | 6.01[−10] |
| $3d$ | 1.60[−23] | 2.67[−17] | 2.77[−11] | 3.59[−11] | | 9.38[−11] | 8.25[−12] | 3.99[−11] |
| $4s$ | 1.61[−24] | 4.46[−18] | 4.46[−12] | 3.07[−12] | 1.15[−09] | | 4.88[−11] | 4.36[−11] |
| $4p$ | 1.47[−25] | 3.05[−19] | 1.93[−13] | 1.93[−13] | 4.76[−11] | 2.31[−11] | | 1.77[−11] |
| $Li^+ + H^-$ | 3.44[−19] | 4.30[−13] | 5.24[−08] | 3.41[−08] | 3.46[−09] | 3.09[−10] | 2.66[−10] | |


[1] S. C. O. Glover, J. Chluba, S. R. Furlanetto, J. R. Pritchard, and D. W. Savin, Adv. At. Mol. Opt. Phys. **63**, 135 (2014).

[2] P. C. Stancil, S. Lepp, and A. Dalgarno, Astrophys. J. **458**, 401 (1996).

[3] E. Bougleux and D. Galli, MNRAS **288**, 638 (1997).

[4] D. Galli and F. Palla, Astron. Astrophys. **335**, 403 (1998).

[5] B. D. Fields, Annu. Rev. Nucl. Part. Sci. **61**, 47 (2011).

[6] F. Spite and M. Spite, Astron. Astrophys. **115**, 357 (1982).

[7] M. Steffen, R. Cayrel, E. Caffau, P. Bonifacio, H.-G. Ludwig, and M. Spite, Memorie della Società Astronomica Italiana (Mem. S.A.It.) **75**, 282 (2008); arXiv:1206.2239 v1 [astro-ph.SR].

[8] E. X. Wang, T. Nordlander, M. Asplund, A. M. Amarsi, K. Lind, and Y. Zhou, MNRAS **500**, 2159 (2020).

[9] D. A. Varshalovich, A. V. Ivanchik, S. A. Balashev, and P. Petitjean, Phys. Usp. **53**, 397 (2010).

[10] C. Pitrou, A. Coc, J.-P. Uzan, and E. Vangioni, Phys. Rep. **754**, 1 (2018).

[11] J. G. Hernández, P. Bonifacio, E. Caffau, H.-G. Ludwig, M. Steffen, L. Monaco, and R. Cayrel, Astron. Astrophys. **628**, A111 (2019).

[12] B. D. Fields, Nature **587**, 203 (2020).

[13] B. D. Fields, K. A. Olive, T.-H. Yeh, and C. Young, J. Cosmol. Astropart. Phys. 03 (2020) 010.

[14] M. Gai, E. E. Kading, M. Hass, K. M. Nollett, S. R. Stern, T. Stora, and A. Weiss, in *European Physical Journal Web of Conferences*, European Physical Journal Web of Conferences, Vol. 227 (2020), p. 01007.

[15] P. Molaro, G. Cescutti, and X. Fu, MNRAS **496**, 2902 (2020).

[16] S. Starrfield, M. Bose, C. Iliadis, W. R. Hix, C. E. Woodward, and R. M. Wagner, Astrophys. J. **895**, 70 (2020).

[17] M. Asplund, ARAA **43**, 481 (2005).

[18] P. S. Barklem, A&ARv **24**, 9 (2016).

[19] W. Steenbock and H. Holweger, Astron. Astrophys. **130**, 319 (1984).

[20] P. S. Barklem, A. K. Belyaev, M. Guitou, N. Feautrier, F. X. Gadéa, and A. Spielfiedel, Astron. Astrophys. **530**, A94 (2011).

[21] T. Launoy, J. Loreau, A. Dochain, J. Liévin, N. Vaeck, and X. Urbain, Astrophys. J. **883**, 85 (2019).

[22] B. Peart and S. J. Foster, J. Phys. B **20**, L691 (1987).

[23] B. Peart and D. A. Hayton, J. Phys. B: At., Mol. Opt. Phys. **27**, 2551 (1994).

[24] G. Eklund, J. Grumer, S. Rosén, M.C. Ji, N. Punnakayathil, A. Källberg, A. Simonsson, R. D. Thomas, M. H. Stockett, P. Reinhed, P. Löfgren, M. Björkhage, M. Blom, P. S. Barklem, H. Cederquist, H. Zettergren, and H. T. Schmidt, Phys. Rev. A **102**, 012823 (2020).

[25] J. T. Lin, T. F. Jiang, and C. D. Lin, J. Phys. B: At., Mol. Opt. Phys. **29**, 6175 (1996).

[26] H. Croft, A. S. Dickinson, and F. X. Gadéa, MNRAS **304**, 327 (1999).

[27] H. Croft, A. S. Dickinson, and F. X. Gadéa, J. Phys. B: At. Mol. Opt. Phys. **32**, 81 (1999).

[28] A. K. Belyaev and Y. V. Voronov, Astrophys. J. **868**, 86 (2018).

[29] P. S. Barklem, A. M. Amarsi, J. Grumer, G. Eklund, S. Rosén, M. Ji, H. Cederquist, H. Zettergren, and H. T. Schmidt, Astrophys. J. **908**, 245 (2021); arXiv:1306.6426v1 [astro-ph.SR].

[30] A. K. Belyaev, J. Grosser, J. Hahne, and T. Menzel, Phys. Rev. A **60**, 2151 (1999).

[31] A. K. Belyaev, P. S. Barklem, A. S. Dickinson, and F. X. Gadéa, Phys. Rev. A **81**, 032706 (2010).

[32] A. K. Belyaev, P. S. Barklem, A. Spielfiedel, M. Guitou, N. Feautrier, D. S. Rodionov, and D. V. Vlasov, Phys. Rev. A **85**, 032704 (2012).

[33] M. Guitou, A. Spielfiedel, D. S. Rodionov, S. A. Yakovleva, A. K. Belyaev, T. Merle, F. Thevenin, and N. Feautrier, Chem. Phys. **462**, 94 (2015).

[34] A. K. Belyaev, D. V. Vlasov, A. Mitrushchenkov, and N. Feautrier, MNRAS **490**, 3384 (2019).

[35] A. K. Belyaev, Phys. Rev. A **88**, 052704 (2013).

[36] P. S. Barklem, Phys. Rev. A **93**, 042705 (2016).

[37] P. S. Barklem, Phys. Rev. A **95**, 069906(E) (2017).

[38] R. E. Olson, F. T. Smith, and E. Bauer, Appl. Optics **10**, 1848 (1971).

[39] A. K. Belyaev and S. A. Yakovleva, Astron. Astrophys. **606**, A147 (2017).

[40] J. Grosser, T. Menzel, and A. K. Belyaev, Phys. Rev. A **59**, 1309 (1999).

[41] A. K. Belyaev, Phys. Rev. A **82**, 060701(R) (2010).

[42] A. K. Belyaev and O. V. Lebedev, Phys. Rev. A **84**, 014701 (2011).

[43] A. K. Belyaev, Phys. Rev. A **48**, 4299 (1993).

[44] S. A. Yakovleva, Y. V. Voronov, and A. K. Belyaev, Astron. Astrophys. **593**, A27 (2016).

[45] A. K. Belyaev, Y. V. Voronov, S. A. Yakovleva, A. Mitrushchenkov, M. Guitou, and N. Feautrier, Astrophys. J. **851**, 59 (2017).
[46] A. K. Belyaev, Y. V. Voronov, A. Mitrushchenkov, M. Guitou, and N. Feautrier, MNRAS **487**, 5097 (2019).
[47] A. K. Belyaev, S. A. Yakovleva, and W. P. Kraemer, MNRAS **501**, 4968 (2021).
[48] A. Kramida, Y. Ralchenko, J. Reader, and NIST ASD Team, NIST Atomic Spectra Database (version 5.6), http://physics.nist.gov/asd (2018)
[49] L. D. Landau, Phys. Z. Sowietunion **1**, 88 (1932).
[50] L. D. Landau, Phys. Z. Sowietunion **2**, 46 (1932).
[51] C. Zener, Proc. Roy. Soc. A **137**, 696 (1932).
[52] See Supplemental Material at http://link.aps.org/supplemental/10.1103/PhysRevA.104.022812 for the complete set of the calculated rate coefficients (in unit of $cm^3\,s^{-1}$) for all partial inelastic processes in lithium-hydrogen collisions for all different isotopes at the temperature range of $T = 1000$–$10\,000$ K.